

# Tube manufacturing trials by different routes in 9CrW-ODS martensitic steels

S. Ukai <sup>a,\*</sup>, T. Narita <sup>a</sup>, A. Alamo <sup>b</sup>, P. Parmentier <sup>b</sup>

<sup>a</sup> Japan Nuclear Cycle Development Institute, O-arai Engineering Center, 4002, Narita-cho, O-arai-machi, Higashi-Ibaraki-gun, Ibaraki-ken, 311-1393, Japan

<sup>b</sup> Nuclear Materials Department, Commissariat à l'Energie Atomique, CEA-Saclay, SRMA, 91191 Gif-sur-Yvette, France

## Abstract

In the collaboration work between JNC and CEA-Saclay, JNC and CEA independently manufactured ODS martensitic cladding tubes by their own fabrication routes. Manufacturing started from the same hollow shape mother tubes with a composition of 9Cr–2W–0.1Ti–0.24Y<sub>2</sub>O<sub>3</sub>. The HPTR cold-rolling process was used by both JNC and CEA, but the applied fabrication routes included different cross-section reduction ratios, number of passes and intermediate heat treatments. The manufactured claddings exhibited an isotropic grain structure and equivalent tensile strength in the longitudinal and transverse directions. Even though different cross-section reduction ratios and intermediate annealing treatments were used, both cladding tubes manufactured by JNC and CEA showed similar levels of tensile and internal creep rupture strength.

© 2004 Elsevier B.V. All rights reserved.

## 1. Introduction

The oxide dispersion strengthened (ODS) ferritic–martensitic steels with superior creep strength above 700 °C are expected to be prospective materials not only for the long-life cladding tubes of the advanced fast reactor fuel elements [1–5] but also for structural materials of blanket systems of DEMO fusion reactors [6–8]. In the collaboration work between Japan Nuclear Cycle Development Institute (JNC) and CEA-Saclay, extensive efforts have been made to study the tube manufacturing processes in 9/12Cr-ODS ferritic–martensitic steels. This paper presents the main results obtained by manufacturing 9CrW-ODS martensitic steel tubes. In JNC/CEA collaboration work, CEA designed the basic composition of 9CrW-ODS martensitic steels, and JNC manufactured the hollow shape mother tubes. Both JNC and CEA independently manufactured cladding tubes through their own fabrication routes to the final

dimensions of 6.55 mm outer diameter, 0.45 mm thickness and 1 m length. The optical and SEM observations, texture determinations, tensile and internally pressurized creep rupture tests were conducted to characterize the manufactured cladding tubes.

## 2. Mother tube manufacturing

Argon gas atomized powder of Fe–0.1C–9.0Cr–2W–0.1Ti (mass%) was mechanically alloyed with yttrium oxide powder by using the attrition type ball mill. The particle size of the atomized powder is less than 150 μm, and 10 kg of powder was mixed with Y<sub>2</sub>O<sub>3</sub> powder for 48 h in an argon gas atmosphere at a rotational speed of 220 rpm. The mechanically alloyed powder was then canned, and degassed at a temperature of 350 °C in a 0.1 Pa vacuum for 2 h. Using a 400 ton press, the cans filled with the mechanically alloyed powder were hot extruded at 1050 °C to make bars of 24 mm diameter. The extruded bars were heat treated at 1050 °C for 1 h, followed by slow furnace cooling at cooling rate of 100 °C/h. The 20 hollow shape mother tubes were

\* Corresponding author. Tel.: +81-29 267 4141x5710; fax: +81-29 267 1676/7130.

E-mail address: [uki@oec.jnc.go.jp](mailto:uki@oec.jnc.go.jp) (S. Ukai).

Table 1  
Chemical composition of CM2 mother tube (mass%)

	C	Si	Mn	P	S	Ni	Cr	Ti	W	N	Y <sub>2</sub> O <sub>3</sub>	Ex.O
Lower	0.08	–	0.4	–	–	–	8.5	–	1.8	0.015	0.20	–
Target	0.10	–	0.5	–	–	–	9.0	0.1	2.0	0.025	0.25	–
Upper	0.12	<0.05	0.6	<0.01	<0.01	<0.05	9.5	≤ 0.1	2.2	0.035	0.27	–
Chemical analysis	0.12	0.03	0.51	0.004	0.002	0.04	9.40	0.09	2.10	0.025	0.24	0.06

Fe: bal.

Ex.O: estimated from total oxygen content minus oxygen coupled with Y<sub>2</sub>O<sub>3</sub>.

prepared from the same number of extruded bars by machining into the dimension of 18 mm outer diameter, 2 mm wall thickness and 350 mm length. The result of chemical analysis of manufactured mother tubes is listed in Table 1, together with specification target and tolerance. The basic composition is Fe–0.10C–9Cr–2W–0.1Ti–0.25Y<sub>2</sub>O<sub>3</sub>, and all of manufactured mother tubes satisfied the specified composition range.

### 3. Cladding tube manufacturing

#### 3.1. JNC route

Table 2 shows the manufacturing process of cladding tubes from the hollow shape mother tubes by JNC route. The HPTR cold rolling was repeated in 11 passes, and the cross-section reduction ratio for each pass is limited to approximately 20%. The first cold rolling of

the mother tube induced a large increase of hardness by about 150  $H_v$ , and the following cold rolling caused small amounts of hardness increase. At intervals of three or four cold-rolling passes, the intermediate heat treatment was conducted at 1050 °C for 1 h followed by slow furnace cooling (FC), in order to soften the cold-rolled tubes. This slow cooling rate of 150 °C/h leads to ferrite formation without martensite phase transformation [9], which reduced the hardness as much as about 50  $H_v$ . The final heat treatment consists of normalizing at 1050 °C for 2 min followed by air cooling (AC), and then tempering at 750 °C for 60 min followed by air cooling. The dimensions of the manufactured cladding were 6.56 mm in outer diameter, 0.45 mm thick and 1m long. The manufactured claddings by JNC route are designated as JNC-CP.

Non-destructive examinations were carried out for 15 manufactured pieces of claddings. The visual inspection revealed shallow scratch on the outer surface of two

Table 2  
Manufacturing route for cladding tubes process used by JNC

Process	Tube size	Rd (%)	Temperature (°C)	Time (min)	Hardness ( $H_v$ )
CM2 mother tubes	18.0 mm OD×2.00 mm TH				278
Cold rolling (1st)	16.5 mm OD×1.77 mm TH	18.4			435
Cold rolling (2nd)	15.1 mm OD×1.55 mm TH	19.9			444
Cold rolling (3rd)	13.6 mm OD×1.35 mm TH	21.0			457
Heat treatment (1st)			1050	60 (FC)	410
Cold rolling (4th)	12.3 mm OD×1.16 mm TH	21.9			457
Cold rolling (5th)	11.1 mm OD×1.00 mm TH	21.9			452
Cold rolling (6th)	10.0 mm OD×0.86 mm TH	22.3			473
Cold rolling (7th)	9.2 mm OD×0.77 mm TH	16.9			464
Heat treatment (2nd)			1050	60 (FC)	414
Cold rolling (8th)	8.4 mm OD×0.68 mm TH	19.9			432
Cold rolling (9th)	7.5 mm OD×0.58 mm TH	22.6			467
Cold rolling (10th)	6.7 mm OD×0.49 mm TH	24.6			464
Heat treatment (3rd)			1050	60 (FC)	380
Cold rolling (11th)	6.60 mm OD×0.48 mm TH	4.4			389
Heat treatment (4th)			1050	2 (AC)	
			750	60 (AC)	368
Polishing	6.56 mm OD×0.45 mm TH				

FC: Furnace cooling.

AC: Air cooling.

pieces of claddings. The ultrasonic testing was conducted over the entirely length of the claddings using a standard cladding tube with calibrated artificial defects of 30  $\mu\text{m}$  depth for both circumferential and axial directions; defects beyond 30  $\mu\text{m}$  were identified in three pieces of claddings. The dimensions of manufactured claddings were precisely measured by the ultrasonic testing method, and the dimensional accuracy of manufactured claddings satisfies the specification limit of  $6.55 \pm 0.030$  mm in outer diameter,  $5.65 \pm 0.030$  mm in inner diameter and wall thickness greater than 0.42 mm.

### 3.2. CEA route

The two kinds of cold-forming processes (cold drawing and HPTR rolling) were tested in the first trial to determine the suitable process to be applied and the allowable maximum cold-working level. HPTR cold rolling was consequently adopted to manufacture ODS martensitic steel cladding, since the cold-drawing process induced early cracking from the first steps of the manufacturing.

Table 3 shows the manufacturing process of cladding tubes by HPTR cold rolling in CEA route. The eight passes were conducted using a cross-section reduction ratio of about 30% for each pass, and intermediate anneals were applied every two passes. Comparing with JNC route shown in Table 2, the HPTR cold rolling by CEA route induces relatively low increase of hardness. The intermediate heat treatment, performed at 800 °C for 2 h in argon gas atmosphere, decreases hardness approximately by only about 20  $H_v$ , which is lower than by furnace cooling after normalization conducted by JNC route. The final heat treatment consists of the normalization at 1100 °C for 15 min under vacuum atmosphere followed by fast cooling to induce the

martensite transformation and the subsequent tempering at 750 °C for 1 h. The hardness of the manufactured cladding approaches that of JNC claddings. The manufactured cladding is designated as CEA-CC2.

Nineteen clad tubes of 1 m length were manufactured and inspected to check their final dimensions and to detect eventual defects and flaws produced during manufacturing. Dimensions were determined by ultrasonic techniques. All tubes satisfied the specifications, except one where the thickness and inner diameter exceeded the required limits. Eddy current inspection, using a calibrated standard defect of 0.3 mm (axial direction)  $\times$  0.25 mm (tangential direction), identified defects in three pieces of cladding tubes.

## 4. Characterization of cladding tubes

### 4.1. Microstructure and texture

Fig. 1 shows optical micrographs of the longitudinal cross-section of the manufactured JNC-CP and CEA-CC2 cladding. The microstructure of both cladding tubes consists of a tempered martensite structure with homogeneous grain morphology, indicating that the elongated grain structure produced during hot-extrusion and cold-rolling processes was destroyed and rearranged by the alpha-to-gamma phase transformations. The stripe-shaped grains (white contrast) observed along the axial rolling direction in JNC-CP cladding could be residual alpha grains that formed during the hot-extrusion process and remained throughout cold rolling and heat treatment without alpha-to-gamma phase transformation [10]. In the CEA-CC2 cladding, some alignments of carbides are also detected parallel to the working direction.

Table 3  
Manufacturing route for cladding tubes process used by CEA

Process	Tube size	Rd (%)	Temperature (°C)	Time (min)	Hardness ( $H_v$ )
<i>CM2 mother tubes</i>	18.0 mm OD $\times$ 2.00 mm TH				280
Cold rolling (1st)	15.2 mm OD $\times$ 1.67 mm TH	30			
Cold rolling (2nd)	12.7 mm OD $\times$ 1.46 mm TH	27			360
<i>Heat treatment (1st)</i>			800	120	347
Cold rolling (3th)	11.5 mm OD $\times$ 1.28 mm TH	20			
Cold rolling (4th)	10.0 mm OD $\times$ 1.04 mm TH	29			355
<i>Heat treatment (2nd)</i>			800	120	337
Cold rolling (5th)	9.0 mm OD $\times$ 0.86 mm TH	25			
Cold rolling (6th)	8.1 mm OD $\times$ 0.75 mm TH	21			355
<i>Heat treatment (3rd)</i>			800	120	328
Cold rolling (7th)	7.3 mm OD $\times$ 0.60 mm TH	27			
Cold rolling (8th)	6.57 mm OD $\times$ 0.465 mm TH	27			357
<i>Heat treatment (4th)</i>			1100	15 (AC)	352
			750	60 (AC)	

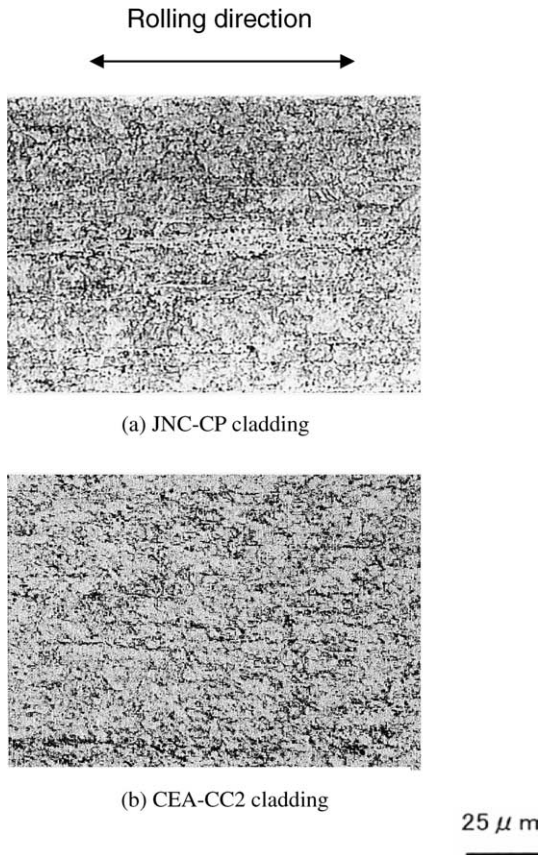


Fig. 1. Optical microstructure of JNC-CP and CEA-CC2 claddings (longitudinal cross-section).

The typical texture for both mother tube and cladding was determined to characterize the degree of anisotropy induced by the manufacturing. The experimental pole figures (110), (200) and (111), orientation distribution functions and the texture sharpness index  $J$  were determined on the transverse cross-section of tubes using the electron back scattering diffraction pattern (EBSP) system available on a SEM. The mother tubes exhibited a  $\langle 110 \rangle$  fiber texture resulting from a tendency of grains to align with  $\langle 110 \rangle$  direction along the axial direction with no preferential orientation in the perpendicular plane. In the cladding tube of CEA-ODS, the initial  $\langle 110 \rangle$  fiber texture had a tendency to decrease, and no clear preferential orientation was obtained. The  $J$ -index, value of 6 in mother tube, was reduced to 2 for cladding tube after cold rolling and final heat treatments.

4.2. Mechanical properties

Tensile tests in the longitudinal and transverse direction of the manufactured cladding tubes were

conducted in the temperature range 20–750 °C. The geometry and dimensions of specimens are described in [2]. Equivalent tensile properties were found in both directions, in particular for the temperature range 450–750 °C as shown in Fig. 2.

In Fig. 3, 0.2% yield stress of JNC-CP and CEA-CC2 claddings, other martensitic steel and ODS steels is compared. It is to be noticed that JNC-CP and CEA-CC2 claddings exhibit almost the same level in 0.2% yield strength. The 9Cr–1Mo is a conventional martensitic steel, and the ODS version 9Cr1Mo–Y<sub>2</sub>O<sub>3</sub> containing 0.25 mass% Y<sub>2</sub>O<sub>3</sub> was manufactured by means

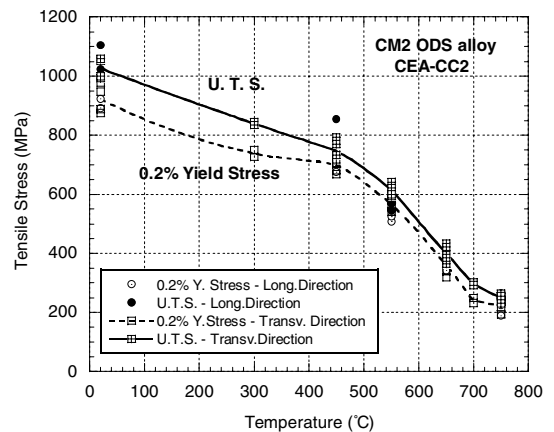


Fig. 2. Tensile properties of CEA-CC2 cladding tubes determined in the longitudinal and transverse directions.

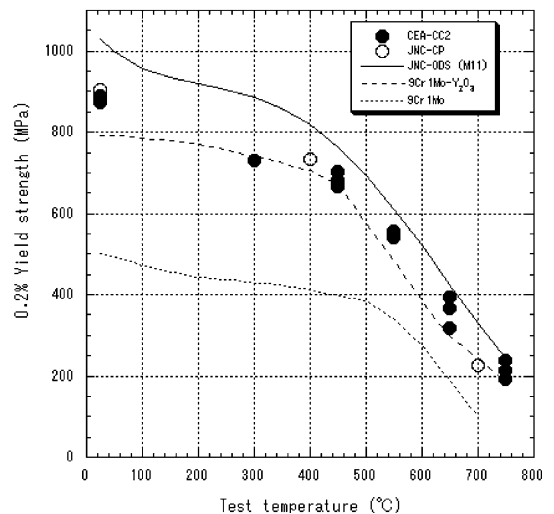


Fig. 3. Comparison of 0.2% yield strength for JNC-CP and CEA-CC2 claddings, 9Cr1Mo conventional steel and different ODS alloys in the transverse direction using ring specimens.

of mechanically alloying and hot extrusion in CEA-Saclay [9]. The JNC-ODS (M11) is a Fe–0.13C–9Cr–2W–0.2Ti–0.35Y<sub>2</sub>O<sub>3</sub> alloy recently manufactured as cladding tubes by four-pass cold rolling using a pilger mill [11]. The final heat treatments consisted on normalizing at 1050 °C for 1 h and tempering at 800 °C for 1 h. From Fig. 3, the Y<sub>2</sub>O<sub>3</sub> addition improves the 0.2% yield stress beyond the conventional 9Cr1Mo. JNC-CP and CEA-CC2 claddings manufactured in this study show almost the same stress level as the 9Cr1Mo–Y<sub>2</sub>O<sub>3</sub>. M11 cladding has superior 0.2% yield stress, associated with larger amount of 0.35 mass% Y<sub>2</sub>O<sub>3</sub> and 0.2 mass% Ti [5].

Fig. 4 shows results of creep rupture tests of JNC-CP and CEA-CC2 claddings obtained at 700 °C, using internally helium gas pressurized specimens in the hoop stress range 90–150 MPa and rupture times up to 7000 h. Again, both type of cladding exhibit similar strength levels and the same trend of hoop stress vs. rupture time. However, CEA-CC2 cladding exhibits slightly longer rupture times than that of JNC-CP cladding due to presumably a more homogeneous microstructure. As a reference, the stepwise increase of creep rupture strength in M11 cladding are also plotted. This improvement in M11 cladding could be attributed to the increase of Y<sub>2</sub>O<sub>3</sub> and Ti addition, which results in the reduced size of Y–Ti–O complex oxide and concomitantly the reduced spacing between oxide particles, although it was pointed out that in the case of ferritic ODS steel the metallurgical and mechanical behaviour are strongly dependent on the working processes by the bias of induced deformation textures [12,13].

It is concluded from this study that similar strength level in tensile and creep rupture properties was attained

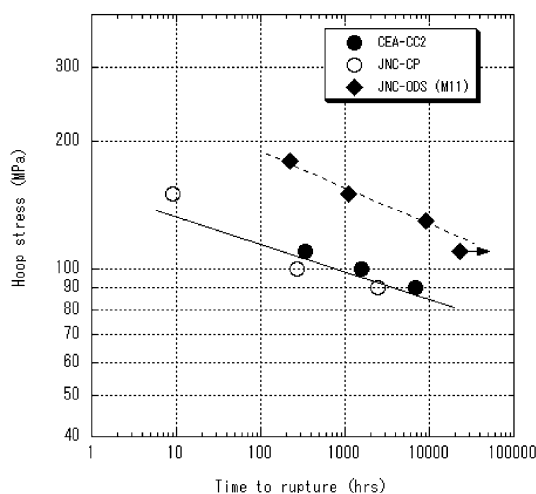


Fig. 4. Comparison of the creep rupture strength determined at 700 °C on pressurized specimens of JNC-CP, CEA-CC2 and JNC-ODS (M11) steels.

for the cladding tubes manufactured by JNC and CEA using HPTR rolling process, not depending on different fabrication routes included different cross-section reduction ratios, number of passes and intermediate heat treatments.

## 5. Conclusion

In the frame of collaboration work, JNC and CEA manufactured thin wall tubes of ODS-9CrW martensitic steel. The main results obtained can be summarized as follows:

- (1) JNC and CEA independently manufactured the claddings from the same mother tubes of 9CrW-ODS martensitic steel using their own fabrication routes to reach the final dimensions of 6.55 mm outer diameter, 0.45 mm thickness and 1 m length. The non-destructive examination was carefully conducted.
- (2) The manufactured cladding tubes exhibited an isotropic grain structure in both longitudinal and transverse cross-sections.
- (3) Equivalent tensile strength levels were obtained along the axial and radial directions of tubes. This is a very important outcome that assesses the isotropic mechanical behaviour of ODS martensitic steels.
- (4) Similar strength levels in tensile and creep rupture properties were attained for the cladding tubes manufactured by JNC and CEA using HPTR rolling processes, not depending on different fabrication routes.

## References

- [1] J.L. Fischer, US Patent 4,075,010 issued 21 February, 1978.
- [2] A. Alamo, J. Decours, M. Pigoury, C. Foucher, Structure application of mechanical alloying, in: Proceedings of an ASM International, 27–29 March 1990.
- [3] T. Yun, L. Guangzu, S. Bingquan, in: 6th Japan–China Symposium on Materials for Advance Energy Systems and Fission & Fusion Engineering, RIAM, Kyushu University 4–6 December 2000.
- [4] S. Ukai, M. Fujiwara, J. Nucl. Mater. 307–311 (2002) 749.
- [5] S. Ukai, S. Mizuta, M. Fujiwara, T. Okuda, T. Kobayashi, J. Nucl. Sci. Technol. 39 (7) (2002) 778.
- [6] R.L. Klueh, D.R. Harries, High-Chromium Ferritic and Martensitic Steels for Nuclear Applications, ASTM Stock Number: MONO 3, 2001.
- [7] D.K. Mukhopadhyay, F.H. Froes, D.S. Gelles, J. Nucl. Mater. 258–263 (1998) 1209.
- [8] R. Lindau, A. Moeslang, M. Schirra, P. Schlossmacher, M. Klimenkov, J. Nucl. Mater. 307–311 (2002) 769.

- [9] V. Lambard, Doctoral thesis, University of Paris XI Orsay, June 2000.
- [10] S. Otsuka, S. Ukai, M. Fujiwara, T. Kaito, T. Narita, these Proceedings.
- [11] S. Ukai, T. Kaito, S. Otsuka, T. Narita, M. Fujiwara, T. Kobayashi, *ISIJ Int.* 43 (12) (2003) 2038.
- [12] A. Alamo, H. Réglé, J.L. Béchade, *Adv. Powder Metall. Part. Mater.* 7 (1992) 169.
- [13] H. Réglé, A. Alamo, in: de Physique (Ed.), *Proc. of the Powder Metallurgy World Congress PM'94, Paris, June 94*, vol. I, p. 507.